This document was prepared in conjunction with work accomplished under Contract No. DE-AC09-76SR00001 with the U.S. Department of Energy.

DISCLAIMER

TECHNICAL DIVISION
SAVANNAH RIVER LABORATORY

DPST-84-726

ACC. NO. 146250

DISTRIBUTION

R. M. HARBOUR, M-6600, AED*
J. E. CONAWAY, M-6600, AED*
J. W. STEWART, M-6600, AED*
S. MIRSHAK, M-6600, AED*
L. W. PATRICK, M-6600, AED*
J. T. GRANAGHAN, 703-A
J. L. WOMACK, 703-A, A-218*
G. F. MERZ, 703-A, A-239
S. D. HARRIS, 773-A
L. R. JONES, 100-L
L. H. MEYER, 703-A*
D. B. SHELDON, 703-A*
C. P. ROSS, 703-A, 5-A*
J. D. SPENCER, 703-A
H. F. ALLEN, 707-C*
W. B. DASPIT, 707-C*
D. R. MUHLBAIER, 704-L
J. T. LOWE, 773-A*
J. L. CRANDALL, 773-A*
L. HIBBARD, 773-A
T. V. CRAWFORD, 773-A*
D. E. STEPHENSON, 773-A
J. F. PROCTOR, 773-A
M. R. BUCKNER, 773-A
A. J. GARRETT, 786-1A
J. P. MORIN, 773-23A*
D. A. SHARP, 773-41A*
SRL RECORDS (4)

August 28, 1984

TO: M. R. BUCKNER

FROM: BARRY S. JOHNSTON AND MARTHA A. McLAIN BSJ

SRL FILE
RECORD COPY

EXPERIMENTAL MODEL OF THE L-AREA OUTFALL

INTRODUCTION

Among the many tasks involved in the restart of the L-area reactor is the need to provide for thermal mitigation of the reactor effluent cooling water. A once-through cooling lake has been chosen for this purpose. This alternative provides satisfactory cooling performance and thermal buffering, with moderate construction time, cost, and maintenance. It is likely, however, that the cooling lake will fail to meet South Carolina environmental requirements during the summer months. In this event, the Savannah River Plant will reduce reactor power until supplemental cooling can be provided. To minimize this further expense and delay, it is desirable to realize the best performance possible from the cooling lake.

SUMMARY

The DuPont Engineering Department has designed an outfall scheme for the proposed L-area reactor effluent cooling lake. It comprises various baffles and a weir added to the existing structure. A 1/24 scale model of this outfall has been built and operated in the Heat Transfer Laboratory. Thermal and visual observations were used to study the vertical mixing which takes place when the hot reactor effluent enters the cooler lake. Since mixing adversely affects lake performance, several alternative outfall concepts were tested. It is recommended that the Wilmington design be modified by adding a sloped ramp to the weir to reduce mixing at the entrance to the lake.

BACKGROUND

The general behavior of a cooling lake is indicated in Fig. 1. The hot water enters at a rate Q from an outfall and mixes with cooler lake water before flowing away over the surface at a rate $D_v Q$ [Adams, 1983]. This mixing is responsible for the underflow of cool water toward the outfall at a rate $(D_v-1)Q$. D_v is a number greater than 1; the larger it is, the larger is the amount of so-called "vertical mixing" which occurs at the outfall. Away from this inlet mixing region, the lake exhibits a stratified countercurrent flow structure with minimal mixing between hot and cold layers. This is indicated by the velocity and temperature profiles shown in the figure.

The primary heat loss from a cooling lake occurs at its surface rather than through the ground. As a consequence, the rate of heat transfer, or the "lake performance", is improved if the inlet energy is contained in a thin hot surface layer of water rather than a thicker, less hot layer. It is obvious that a large value of D_v, indicating much mixing with cooler water, implies a thick layer of outflowing water at a reduced temperature. Hence, one objective in the design of an outfall is the minimization of mixing.

Fig. 2 presents topographical data for the outfall region [Baldwin and Cranston, 1984]. If the lake boundary is assumed to be along the 190 ft contour [Murphy, 1984], it can be seen that the outfall will be characterized by a relatively deep channel flanked by broad shallow shelves. There is, therefore, good reason to expect cold water to be able to penetrate up to the outfall. This means that questions of mixing and outfall performance are pertinent to L-area.

Engineering Department in Wilmington has proposed an outfall design as shown in Fig. 3 [Murphy, 1984]. This design has the

virtue of requiring a relatively minor amount of modification to the existing outfall structure. It features an impingement baffle to break the forward momentum of the flow and directing baffles to aid the spread of the flow over the full width of the weir. To ensure optimum cooling performance for the lake, a decision was made by SRL to construct a physical model of the outfall, and, if possible, to improve Wilmington Engineering's design. The model was constructed and operated in the Heat Transfer Laboratory.

PRINCIPLES OF MODELING

The first criterion to satisfy in a model study is that of geometric similarity; therefore, a model of the outfall shown in Fig. 3 was built to scale. A reduction of 1/24 was chosen so that the model would be a convenient size for the laboratory. The width of the weir was thus 40 inches. By contrast, no attempt was made to reproduce the detailed terrain of the lake. Since the mixing occurs near the outfall, it was considered sufficient to represent the lake by a channel of scaled width and depth, long enough to allow the mixing to be completed, and flanked by shallow submerged shelves. The remainder of the lake, featuring slow stratified flow, would be insensitive to details of terrain. In the experiment, the inlet mixing was generally observed to be concluded at a distance of 4 to 5 pond depths from the inlet, justifying this choice.

Next, operating conditions must be chosen to achieve dynamic similarity between the model and prototype. If one writes the continuity, momentum, and energy equations for buoyancy-stratified single phase flow, simplifies them by considering density variation only in the gravity term (the so-called Boussinesq approximation), and non-dimensionalizes them with suitable reference scales, one finds that the (dimensionless) coefficients in the equations are the Reynolds, Prandtl, and densimetric Froude numbers. These are defined as follows; the above procedure is detailed in Appendix A.

$$Re = \frac{HV}{\nu}$$

$$Pr = \frac{C\,\nu\rho}{k}$$

$$Fr = \frac{\rho_o V^2}{(\rho_o - \rho)\,g\,H}$$

where

H = reference length

V = reference velocity

ν = kinematic viscosity of fluid

ρ = density of fluid

ρ_o = reference density of fluid

C = heat capacity of fluid

k = thermal conductivity of fluid

g = acceleration due to gravity

If experimental conditions can be chosen such that the model has the same dimensionless groups as the prototype, then model and prototype are described by identical equation sets. Further, identical boundary conditions result from geometric similarity; then, it is argued, the behavior of the model is indicative of that of the prototype.

The Prandtl number depends only on fluid properties, and thus does not differ greatly from the L-area prototype to the model. The Froude number, by virtue of the density difference in the denominator, can be varied as needed for the model in order to achieve similarity. In the Reynolds number, however, a decrease in the length scale must be offset by an increase in the fluid velocity or a decrease in the kinematic viscosity of the fluid. One is forced to use excessive flow rates or work with a different fluid. It is virtually impossible to attain a complete dynamic scaling in this situation, and so a choice must be made among dimensionless numbers.

Consider that the mixing of the fluid near the inlet weir is a result of opposing forces. The inertia of the inflowing hot water tends to promote mixing; the buoyancy force between the hot and cold layers aids stratification. The balance of these forces is characterized by the densimetric Froude number, and thus this might be expected to be the most important parameter for the evaluation of mixing. If Fr = 0 (no inlet velocity) a density-stratified body of water would be expected to be stable. As Fr increases, the inertia of the inflowing water comes to dominate, resulting in vertical mixing. Note also that the inverse of Fr is known as the Richardson number [Turner, 1973], commonly used in the study of stratified flows.

The Reynolds number, representing the balance between inertial and viscous forces, is generally associated with the degree of turbulence. Since the model did exhibit turbulence, it was assumed that its behavior might not differ in kind but only in

degree from that of the prototype. Based on these considerations, it was decided to scale by Froude number and not by Reynolds number. If this rationale is valid, the model may not predict the actual performance of a given outfall design, but can allow the better of two to be identified.

Referring to Figure 3, if V is chosen to be the inlet flow rate (170,000 gpm) divided by the cross section available for flow over the inlet weir (80 x 4.5 ft^2), H is taken as the depth of the lake (8 ft), and ρ is calculated between 162 and 90 deg F, the prevailing densimetric Froude number for the L-area outfall becomes 0.232. Convenient corresponding laboratory conditions at 1/24 scale were a flow rate of 21 gpm at 95 deg F into a lake at 82 deg F.

DESCRIPTION OF EXPERIMENT

The outfall model was constructed from half-inch thick polycarbonate sheets. The receiving pond was made from quarter-inch aluminum sheet. Plywood boxes were submerged on either side of the pond to form a central channel 40 inches wide. The depth of water over the boxes varied between 0 and 0.75 inches. The water level in the pond, nominally 4 inches, was controlled by the height of an outlet overflow weir opposite the outfall. The inlet water was heated by means of a stainless steel tube connected between the bus bars of the Heat Transfer Laboratory rectifier system.

In a cooling lake, the temperature of the outflowing water decreases with distance from the outfall; the stream finally turns downward at the opposite end to return as an underflow. The model was much too small to experience any cooling, so the underflow was simulated by introducing a cold water backflow just below the overflow weir through a perforated pipe. A schematic diagram of the apparatus appears in Fig 4, and a photograph of the model is shown in Fig 5.

The flow behavior was studied by dye injection and temperature measurements. Both black waterproof and blue washable inks were used as dye tracers. Each served well, the latter being less murky. The ink was injected via hypodermic tubing from a syringe. This allowed an understanding of the flow field, as well as a rough estimate of the vertical penetration of the incoming fluid. Four type K thermocouples were mounted on a vertical rod, as shown in Fig 6. The vertical position of the measuring junctions could be varied by bending the thermocouples or adjusting a screw in the base. The stand was placed obliquely to the flow as shown in Fig 6.

The general procedure was to set the desired flow rates of inlet and backflow water and then bring the inlet stream to the desired temperature. The pond attained a steady state in about 30 minutes. At this point the thermocouple stand was located as desired. After allowing about one minute for any flow disturbances to dissipate, the thermocouples were scanned at 5 s intervals for 45 seconds, after which the average of the scans was recorded for each thermocouple. Two such averages were recorded at each location, after which the thermocouple stand was moved. Temperature data were generally taken along lines parallel to or perpendicular to the outfall weir. The specific operating procedure and safety analysis are available elsewhere [Johnston, 1984a]. The Engineering Department design was examined in this manner, and then a number of modifications were tried. These included a simple elevation of the weir and the addition of various sloping ramps to the weir.

To compare the behavior of one design with that of another, it was desirable to compute the dilution coefficient D_v. D_v is defined in terms of flow rates, which cannot be conveniently measured, but can be obtained from temperature data. If a simple overall energy balance is performed around the mixing region of the cooling lake shown in Fig 1, considering the inlet, underflow, and mixed streams, there results

$$D_v = \frac{T_i - T_b}{T_m - T_b}$$

where T_m = mixed stream temperature

T_i = inlet temperature

T_b = underflow temperature

This equation was used to calculate experimental values of D_v, letting the surface temperature represent the mixed stream temperature. This is an idealization, but does not seriously affect the results. This point is addressed in Appendix B, where a more rigorous derivation and calculation are performed. Within the mixing region, the surface temperature decreases with distance from the weir. D_v is properly calculated at a location where this temperature has become constant.

As mentioned above, the recorded temperatures were averaged over time. Further, several of these time-averaged values were replicated and averaged to calculate D_v for a given experiment. As a result, the uncertainty due to random scatter has been removed, and that which remains is due to differences in

individual thermocouples. The three thermocouples in question were observed to read within 0.1 deg C of each other in an isothermal medium. If the uncertainty in D_v due to a 0.1 deg C uncertainty in the constituent temperatures is calculated, the resulting 95% confidence limits on D_v are $\pm$ 0.05. In no instance was a replicated result observed to exceed this range.

OBSERVATIONS AND RESULTS

It quickly became obvious that the proposed design has some desirable features. Fig 7 is a qualitative depiction of the outfall flow field. The inlet flow encounters the impingement baffle and is directed to the bottom of the outfall. Here it flows along the bottom, toward the weir, reaching the wall at the forward end of the outfall and turning upward. The upwelling flow divides into two portions, one flowing over the weir out into the lake, the other returning toward the inlet pipe. Seeing this, a naive or hasty observer would judge that water was flowing from the pond into the outfall. For most of the cases studied, this behavior was observed in each of the four subcompartments of the outfall. Two salient points are in evidence. First, the outfall acts as an isothermal settling box. The velocity of the inlet water is reduced to make use of the full width of the weir. As noted below, the mixing with cold lake water takes place in the region of the weir and not on a large scale in the outfall structure itself. Second, the hot water is directed to the preferred destination, i.e., up toward the pond surface. This seems a better arrangement than to have the water flowing down a slope into the lake, as is commonly done [Stefan and Hayakawa, 1971].

In contrast to the outfall, the pond is not isothermal. Fig 8 is a plot of pond temperature, at various depths, along the pond centerline. The prevailing inlet temperature is also shown. It can be seen that the surface temperature decreases and the temperature at a depth of 2.5 inches increases with distance. Since the only mechanism for heat transfer and temperature change in the experiment is that of mixing, Fig 8 indicates that mixing has occurred over at least 63% of the depth of the pond in a distance of 8 inches (2 pond depths) from the weir. The bottom layer temperature, at a depth of 3.9 inches, is unchanged with distance.

The velocity profiles in the pond, as indicated qualitatively by dye injection, are like that shown in Fig 1. The hot outflowing stream runs countercurrent to the cold underflow. The underflow is confined to the deep portion of the pond, but the hot water tends to spread out over the shelves to either side of the central channel. This suggests that a portion of the hot outflow is unavailable for mixing, and this is confirmed by the

temperature measurements of Fig 9. In this figure, the temperature is plotted from the center of the channel along a line parallel to the weir, 8 inches (or 2 pond depths) away from it. The lower temperatures in the center of the channel indicate that more mixing has taken place there than at the edge.

The drawback to the proposed design is the backflow of lake water which occurs over the weir. The outflowing hot water does not occupy all the available flow area, allowing cold water to be drawn up and over the weir. Here it is entrained into the outflow, as shown in Fig 10. This is responsible for the difference in the inlet temperature and the pond surface temperature at the weir as was shown in Fig 8.

In an attempt to improve this performance, the outfall was modified to reduce the backflow over the weir, leaving the other features intact. The first idea was to raise the weir; after this sloping ramps were tried. Fig 11 summarizes the various trials and lists the calculated D_v. It can be seen that a modest decrease in flow area improves performance, especially when combined with a sloped ramp.

The best performer, as indicated by the lowest value of D_v, was a sloping ramp 8 inches long, with a minimum flow depth of 1.5 inches. Fig 12 shows the measured temperature profiles; notice that the surface temperature at the edge of the ramp is virtually equal to the inlet temperature. This indicates that this ramp has allowed negligible cold water backflow into the outfall. The qualitative flow field, observed by dye injection, is shown in Fig 13. The upwelling flow separates at the beginning of the ramp, but reattaches before the end, thus allowing only hot water to circulate in the vortex. Note also in Figure 12 that the water at the 2.5 inch depth undergoes little heating with distance. This indicates less vertical mixing than that in the case of Figure 8.

The base experimental conditions were chosen as described previously in an attempt to simulate the prototypical operation. Recognizing that this may vary, the successful modification was tested at varying conditions of flow rate and inlet temperature. The results are presented as a plot of D_v vs Fr in Fig 14. It can be seen that the outfall is reasonably insensitive to operating conditions over a 5-fold range of Fr.

CONCLUSIONS AND RECOMMENDATIONS

In conclusion, the outfall concept advanced by Engineering Department is a good one. Not only does it appear to reduce the inlet velocity effectively, making full use of the weir, but it uses the existing structure advantageously in supplying the hot water to the lake surface. The experiments have shown, however,

that the outfall performance can be further enhanced by the addition of an upward sloping ramp to the weir. This serves to prevent the intrusion of cold water into the outfall, and thus eliminates a source of mixing.

As discussed earlier, the impossibility of a complete dynamic scaling means that the experimental values of D_v may not be directly applied to prototype operation. However, if by incorporating the ramp modification the L-area dilution coefficient D_v can be reduced by about 0.2, it is estimated from numerical modeling of lake performance [Garrett, 1984] that L reactor power can be increased by 15-20 MW annually, or about 40 MW in the summer, still operating under compliance.

It is recommended that the Engineering Department design (Fig 3) be modified to include the ramp shown in Fig 15. The length and elevations shown are those expected to produce optimum performance. By contrast, the suggested thickness of 1 foot is an initial guess; the ramp should be as thin as is possible, consistent with structural integrity. The supports shown may be modified as well, as long as the ramp remains undercut and transverse flow is allowed. The ramp should extend over the full width of the outfall, ideally impinging on the banks of the lake at either side. This recommendation has been previously communicated [Johnston, 1984b].

Work is underway to explore several additional topics. These are noted here and will be reported in a supplementary document.

- The experiments with sloped ramps have used thin metal plates. The recommended design of Fig 15 will be built to scale to examine the effects of a thicker ramp.

- Since performance was observed to improve with increasing ramp length, a 12 inch sloped ramp will be used to see if further improvements are possible. It is not known whether D_v will approach an asymptote or begin to rise as ramp length increases.

- The pond depth will be varied for a single sloped ramp geometry. D_v has been observed to vary with the flow area over sloped ramps, and this further information will provide an opportunity for confirmation. It will also indicate the sensitivity of the outfall performance to this variable.

- The directing baffles will be removed to determine their necessity for acceptable operation.

- Provision will be made to introduce hot water into the pond in a horizontal or downward fashion. The intention is to document a known poor performer to ensure that the results of this study are not erroneously biased to the good.

REFERENCES

E. E. Adams, Analysis of Cooling Ponds used at the Savannah River Plant, consultant's report to R. F. Schwer, 1983.

Baldwin and Cranston, Topographic Map, Cooling Reservoir Site, L-area, Sheet 4, Baldwin and Cranston Associates, Inc., 2 Apr 1984.

A. J. Garrett, personal communication, 1984.

B. S. Johnston, Outfall and Water Tank Experiment: Safety Analysis and Operating Procedure, rev. 2, Heat Transfer Laboratory, 21 May 1984.

B. S. Johnston, letter to C. D. Spencer, 19 July 1984.

W. T. Murphy, "Support Facilities for L-Reactor Dam and Lake", sketch, 18 April, 1984.

J. S. Turner, Buoyancy Effects in Fluids, Cambridge University Press, 1973.

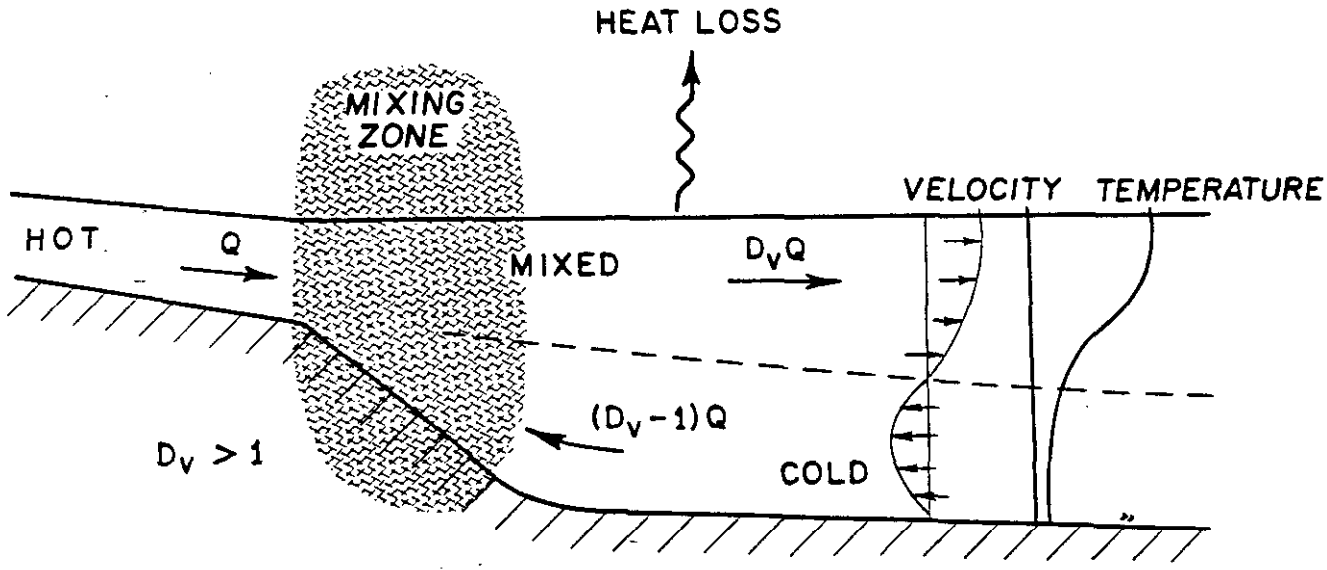

Figure 1. Thermal and hydraulic behavior of a cooling lake.

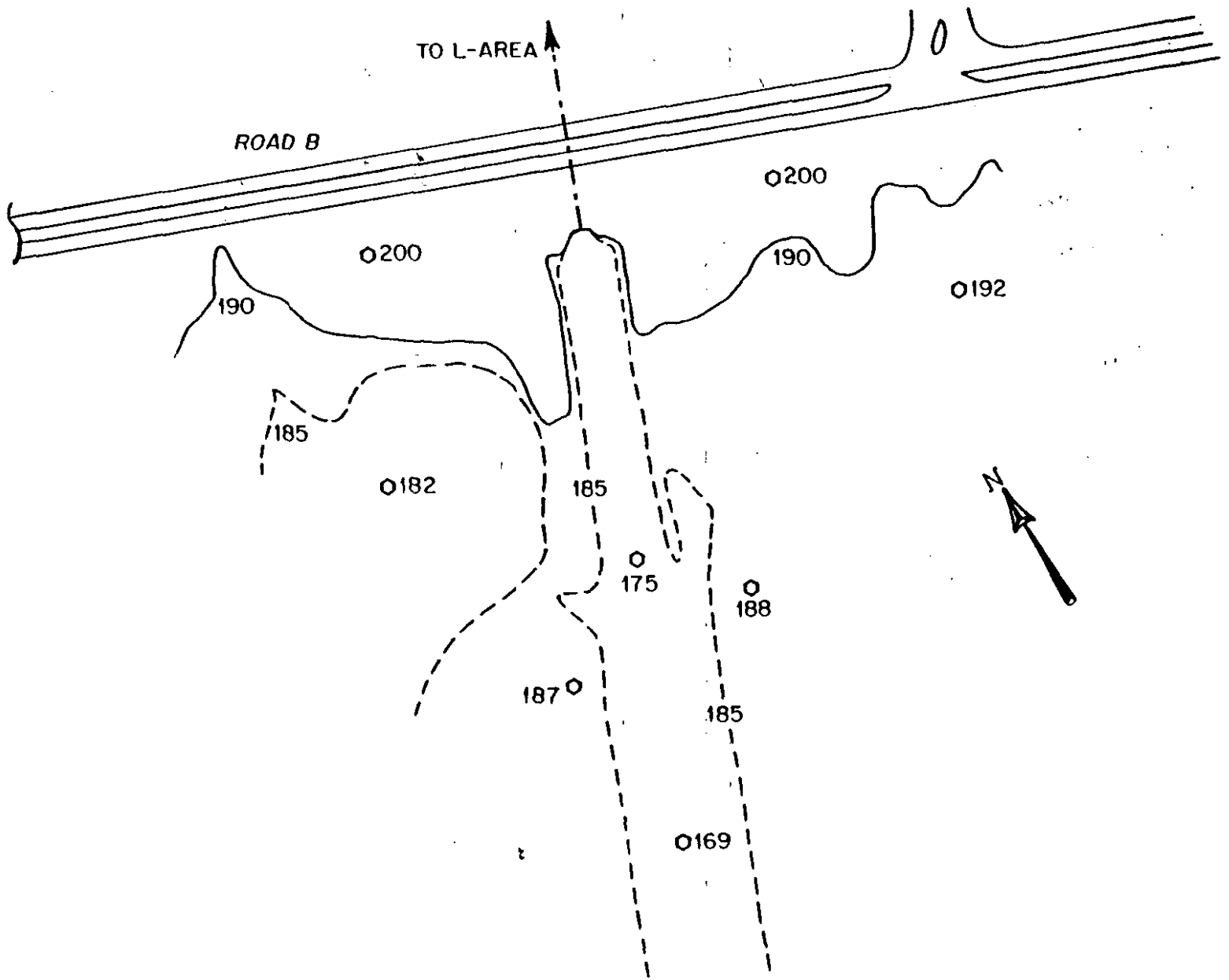

Figure 2. Topographical data for the L-area outfall region.

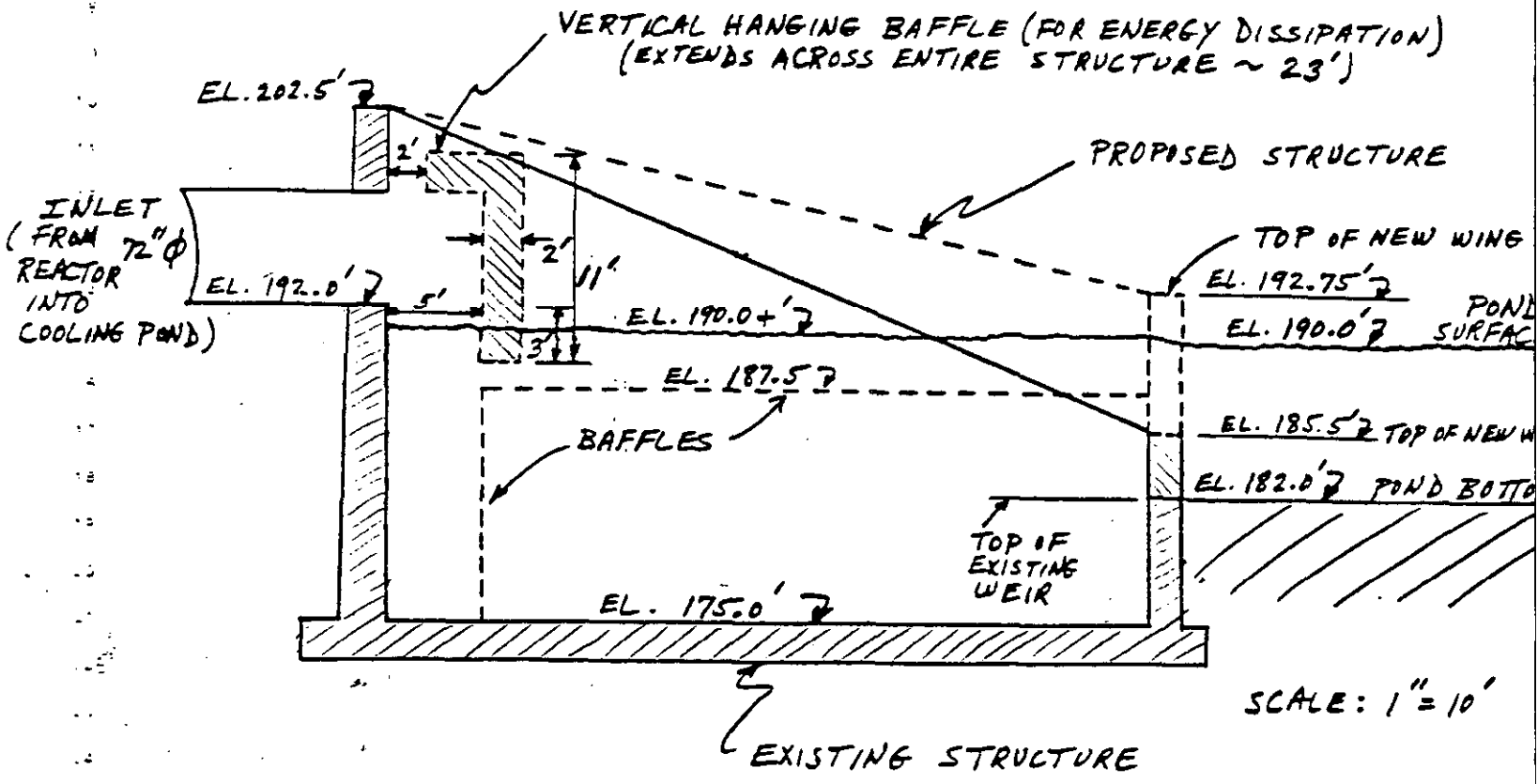

Design Basis for proposed weir structure

Figure 3. Engineering Dept outfall design, elevation. (reproduced from [Murphy, 1984]).

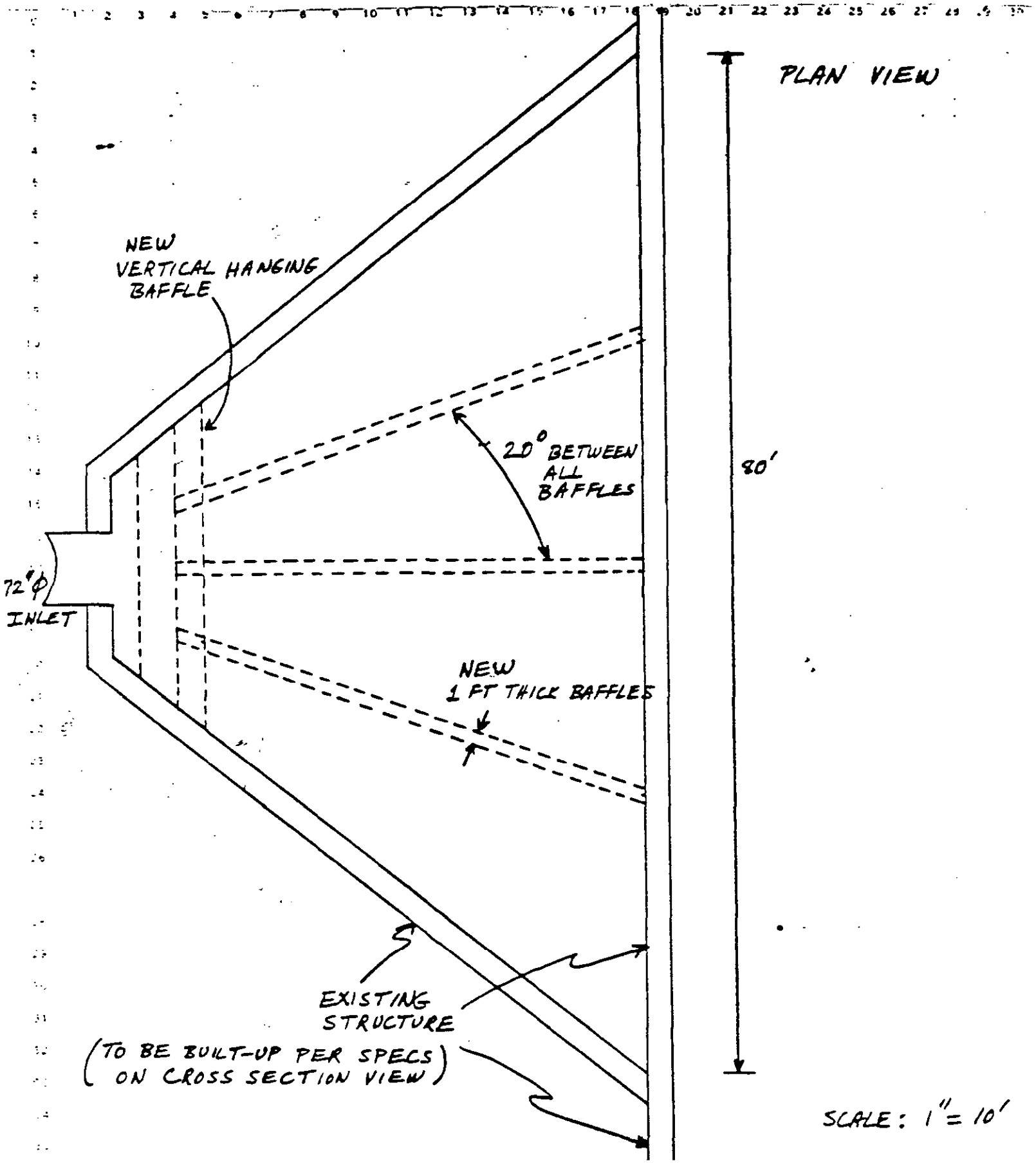

Figure 3. (continued) Engineering Dept. outfall design, plan. (reproduced from [Murphy, 1984])

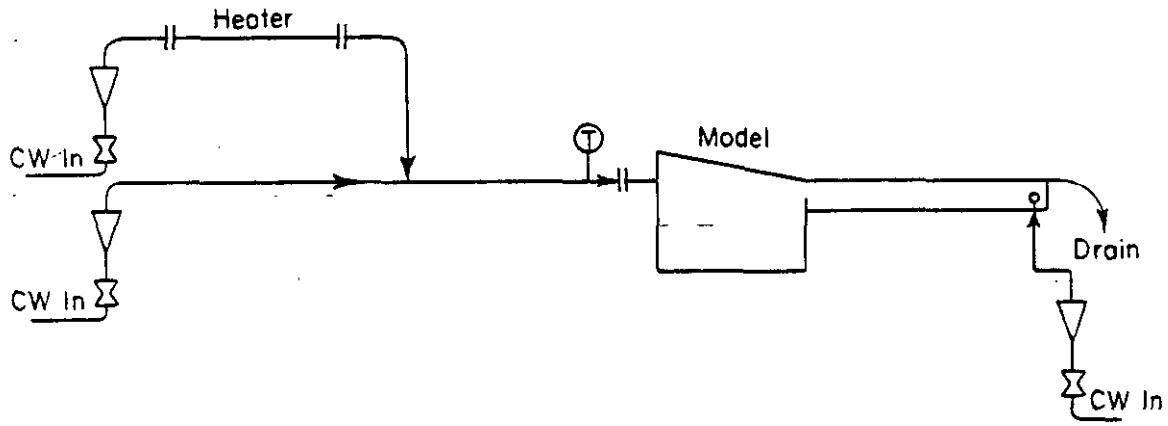

Figure 4. Schematic diagram of outfall model apparatus.

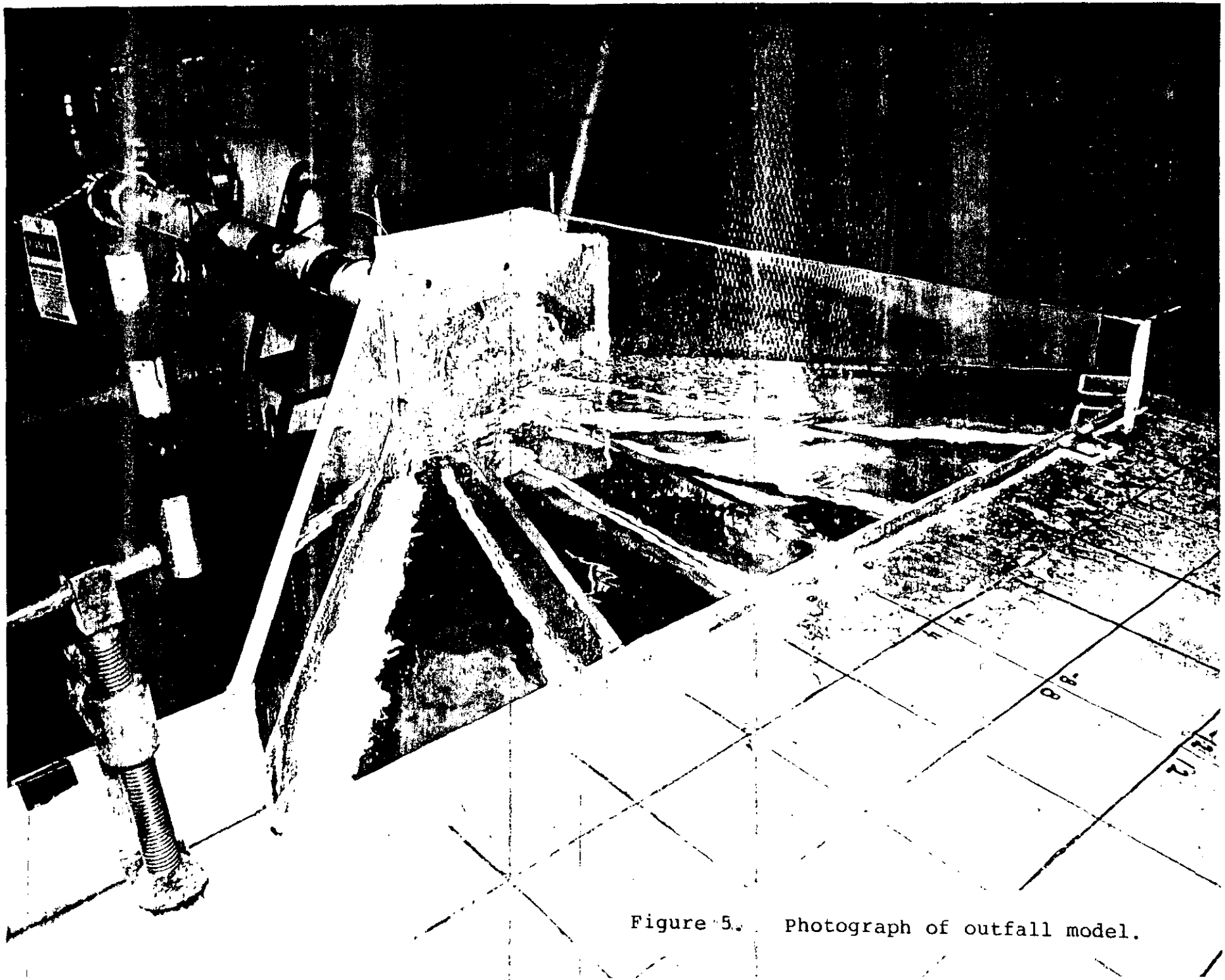

Figure 5. Photograph of outfall model.

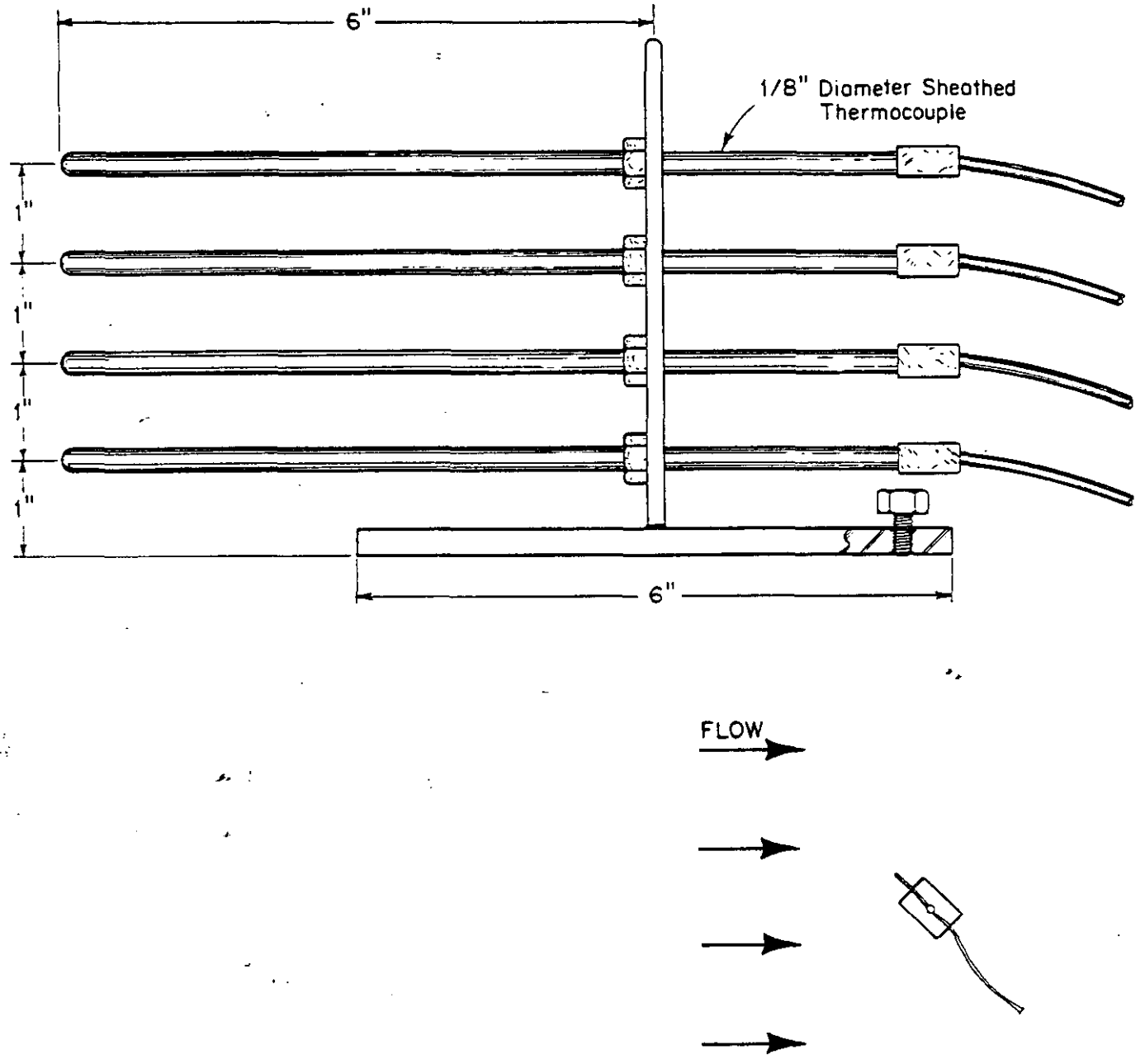

Figure 6. Thermocouple rake; note orientation with respect to flow, shown at bottom.

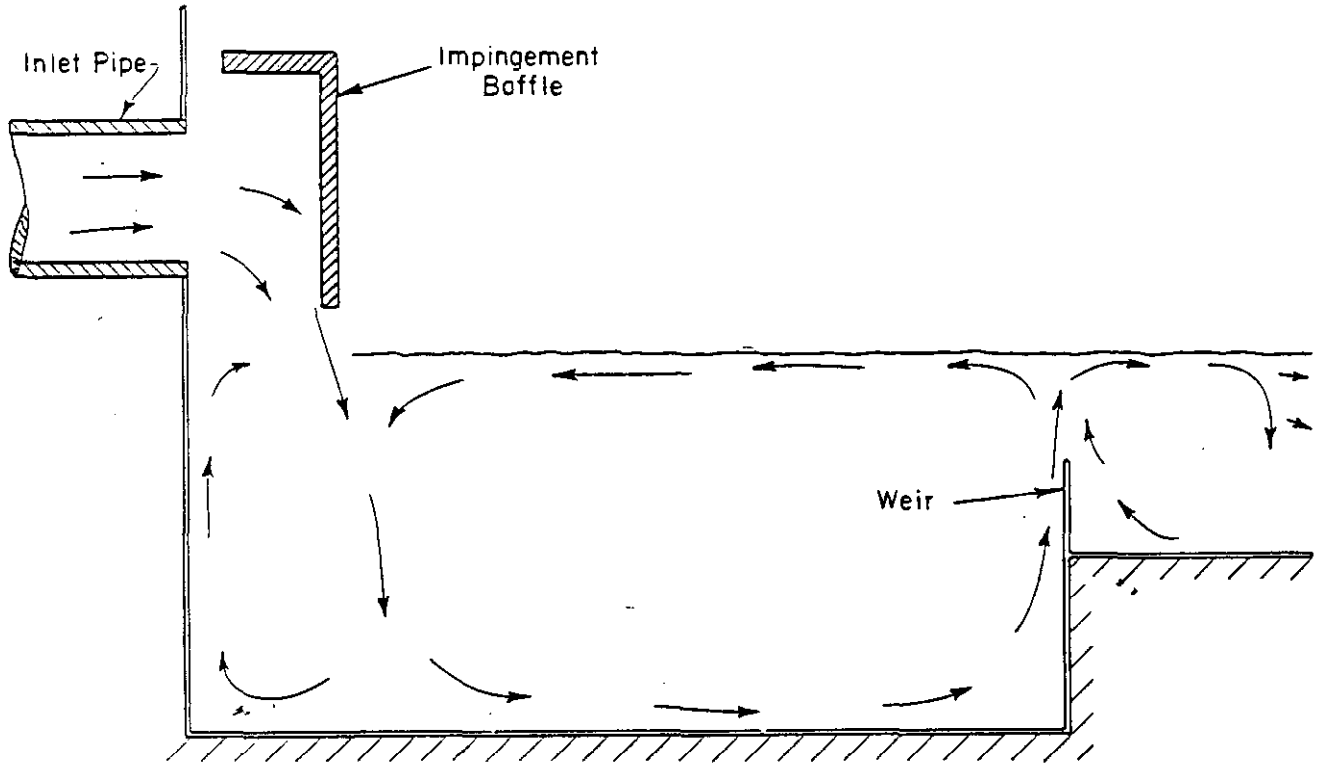

Figure 7. Flow field observed from dye injection in outfall model.

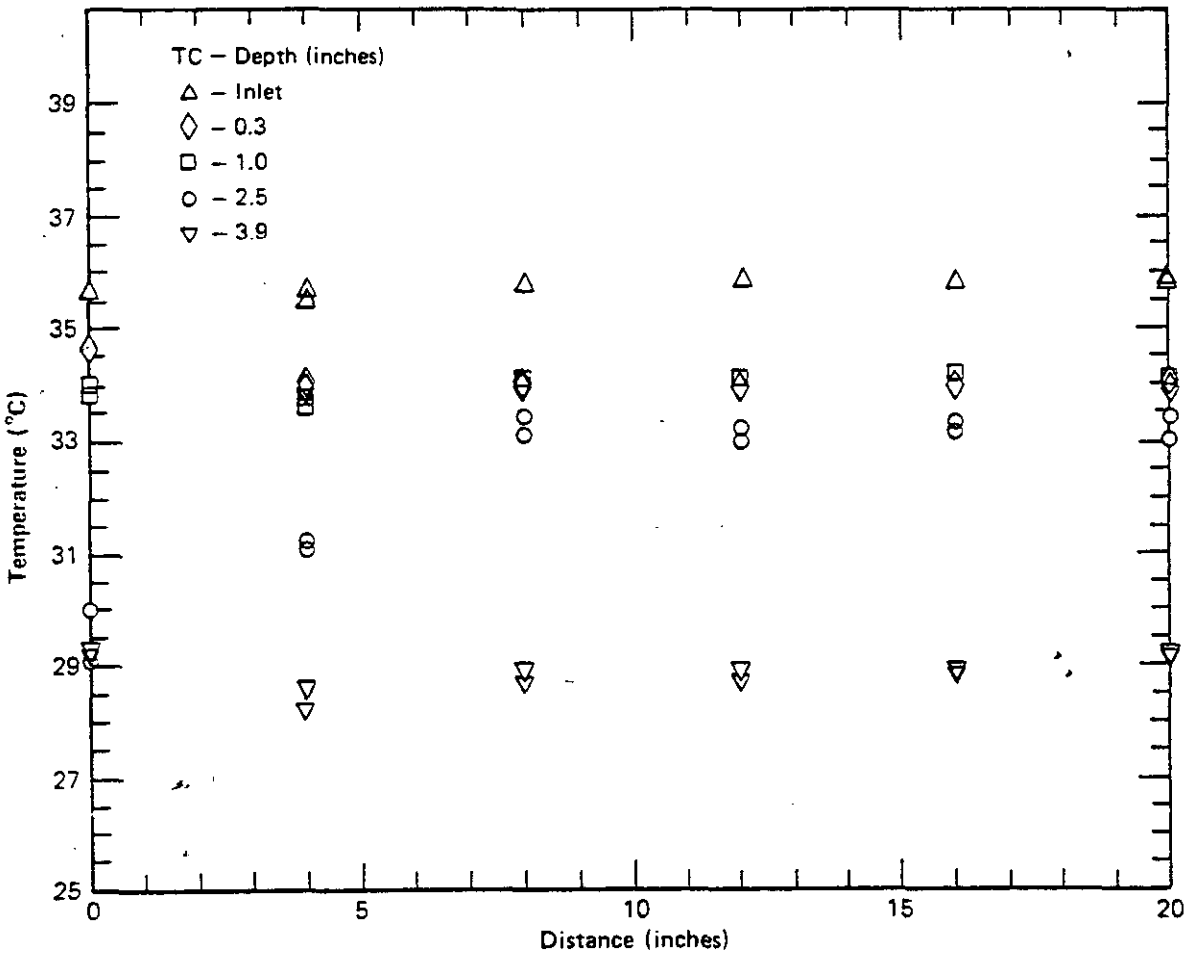

Figure 8. Pond temperature, at various depths, plotted versus the distance from the outfall weir along the pond centerline. (The inlet temperature is measured in the inlet pipe.)

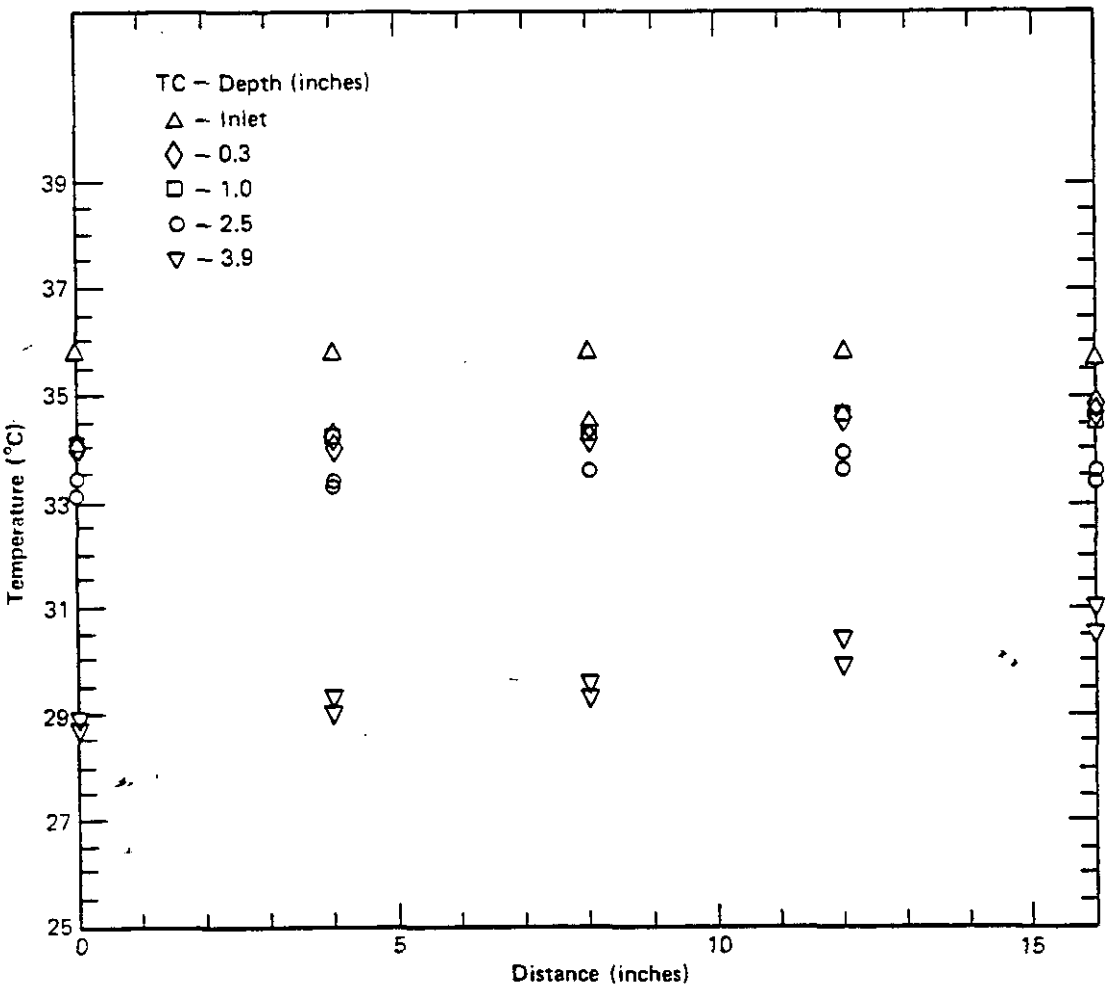

Figure 9. Pond temperature, at various depths, plotted versus the distance from the pond centerline along a line parallel to the outfall weir and eight inches from it. (The inlet temperature is measured in the inlet pipe).

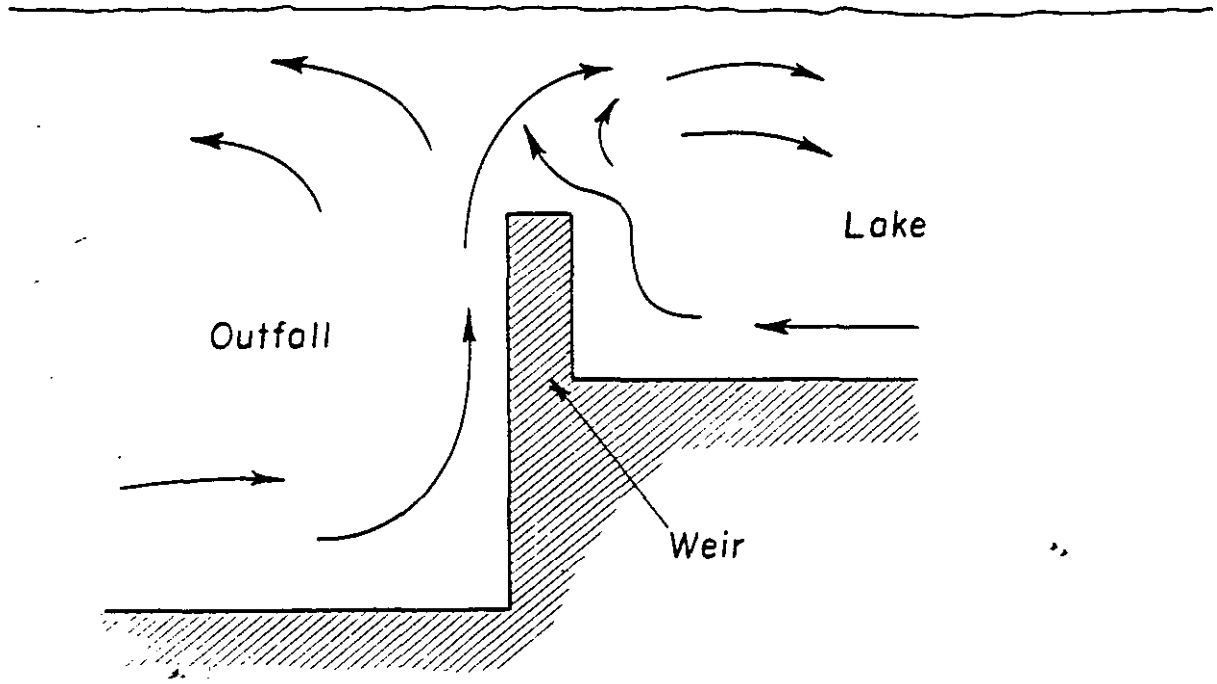

Figure 10. Cool lake-bottom water flows back over the weir, mixing with the outflowing hot stream.

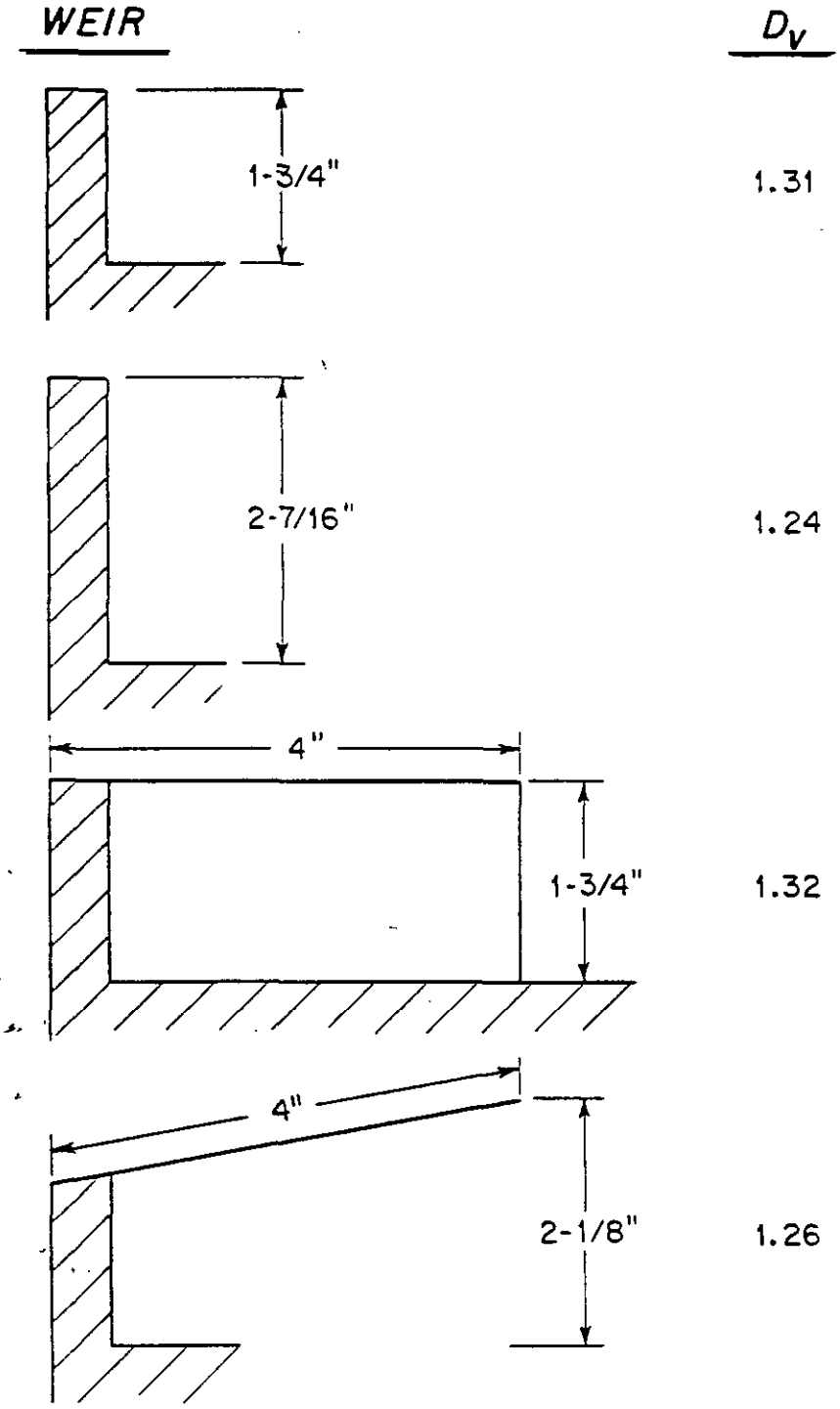

Figure 11. Description of various outfall weir designs and their corresponding experimentally determined values of Dv.

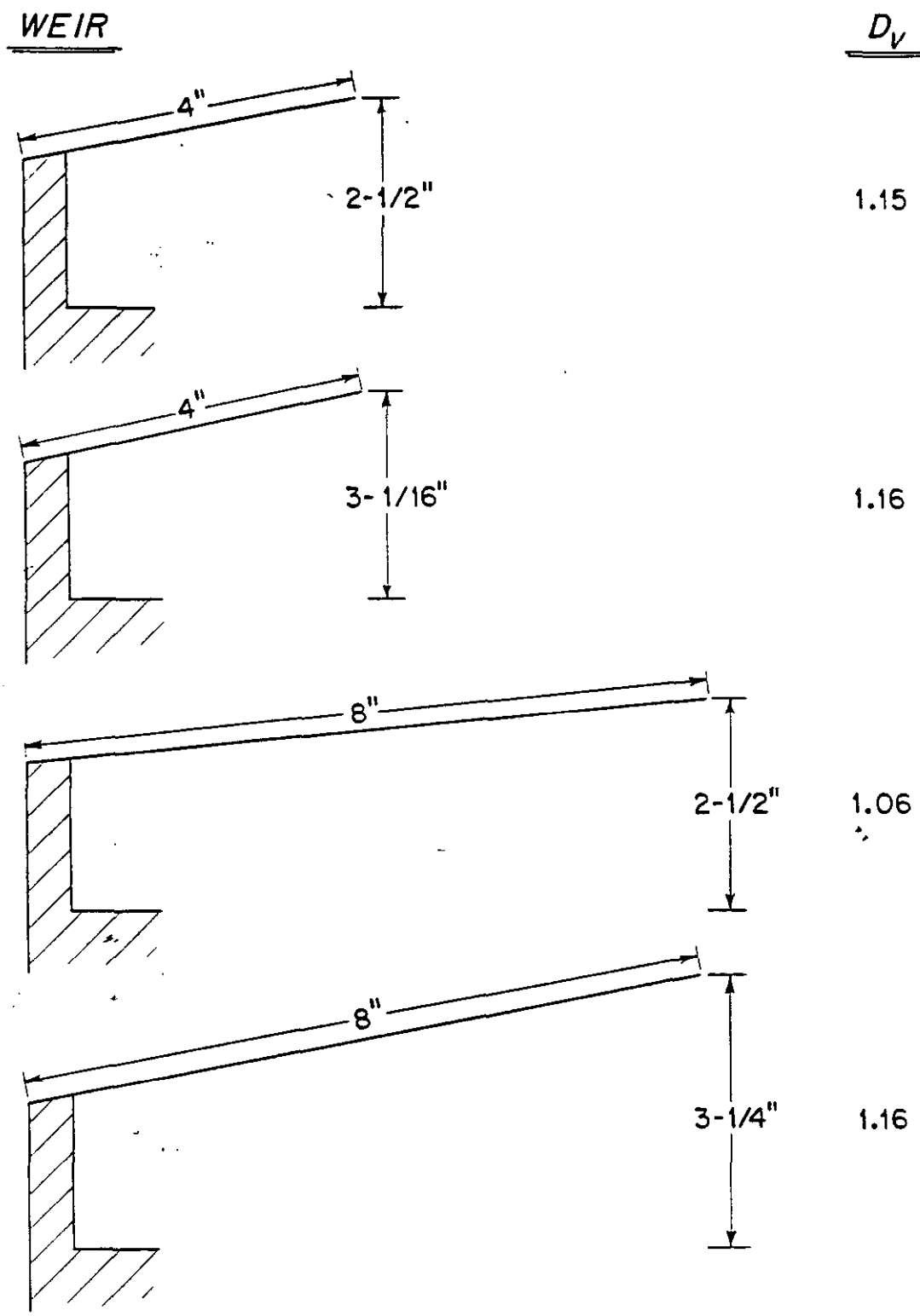

Figure 11. (continued) Description of various outfall weir designs and their corresponding experimentally determined values of Dv.

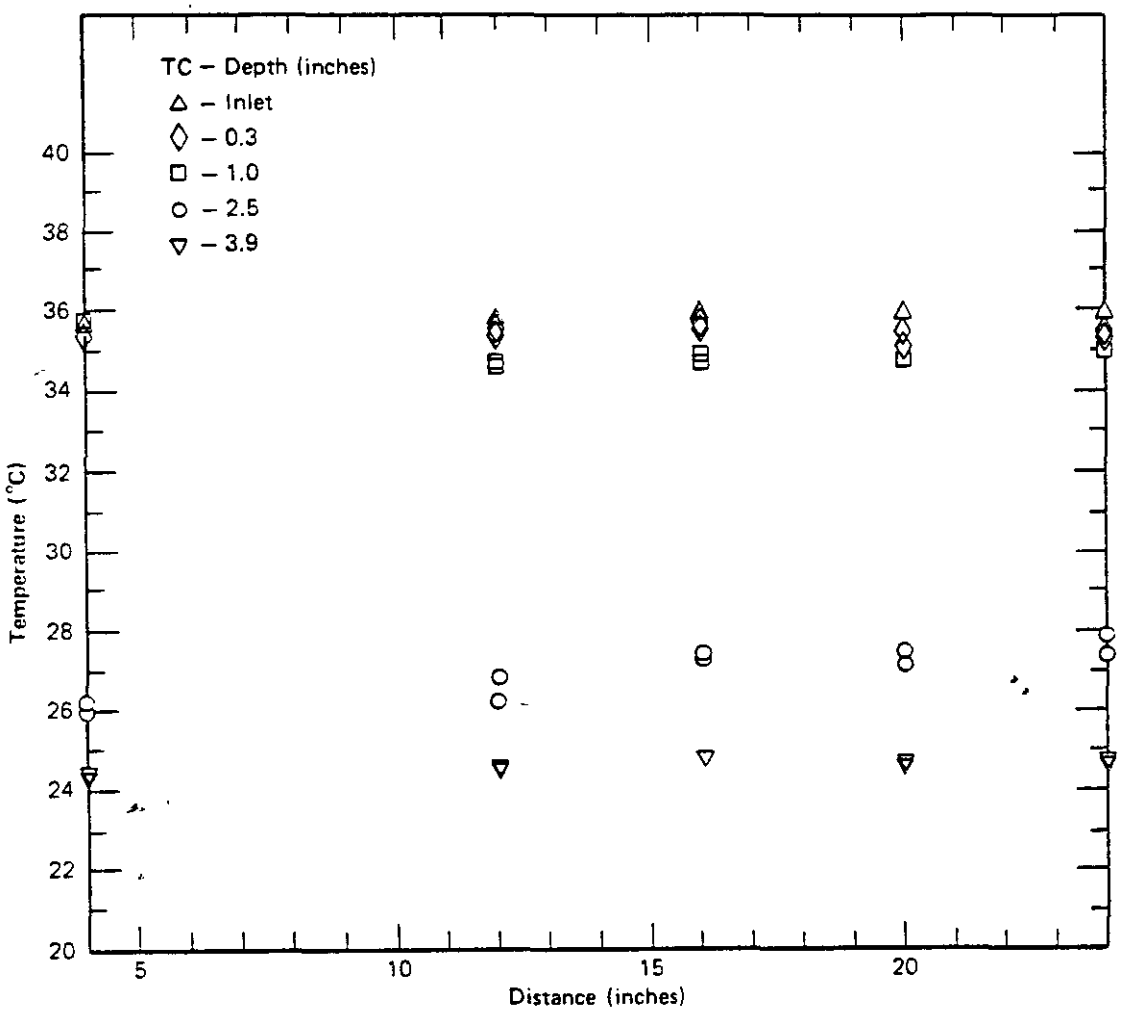

Figure 12. Pond temperature, at various depths, plotted versus the distance from the end of the sloped ramp along the pond centerline. (The inlet temperature is measured in the inlet pipe.)

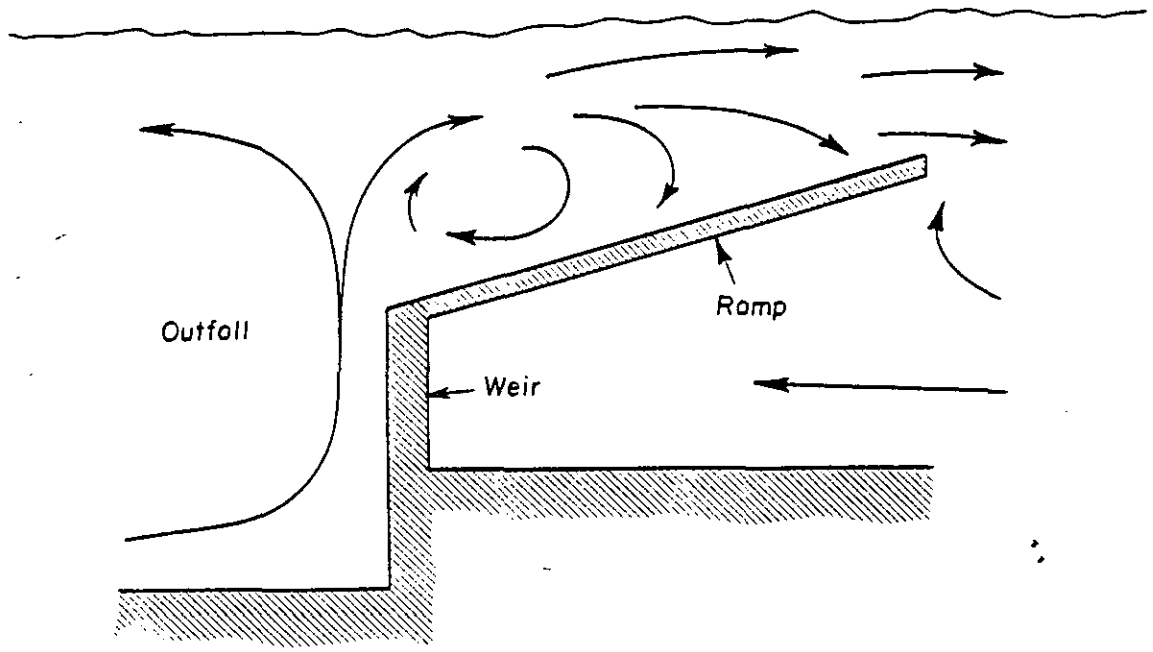

Figure 13. The sloping ramp prevents cool lake-bottom water from flowing back over the weir, reducing mixing with the outflowing hot stream.

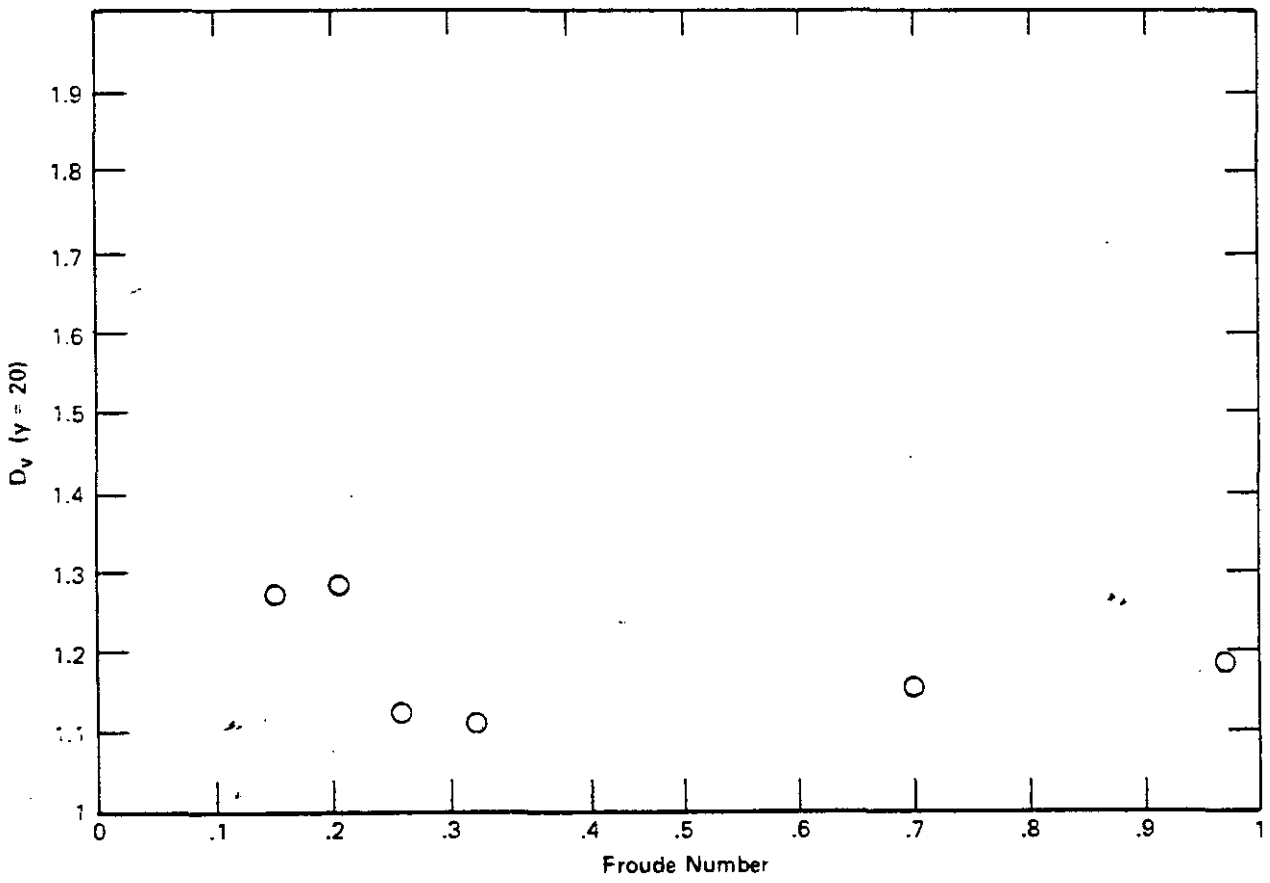

Figure 14. The sloped ramp dilution coefficient Dv, plotted versus the densimetric Froude number.

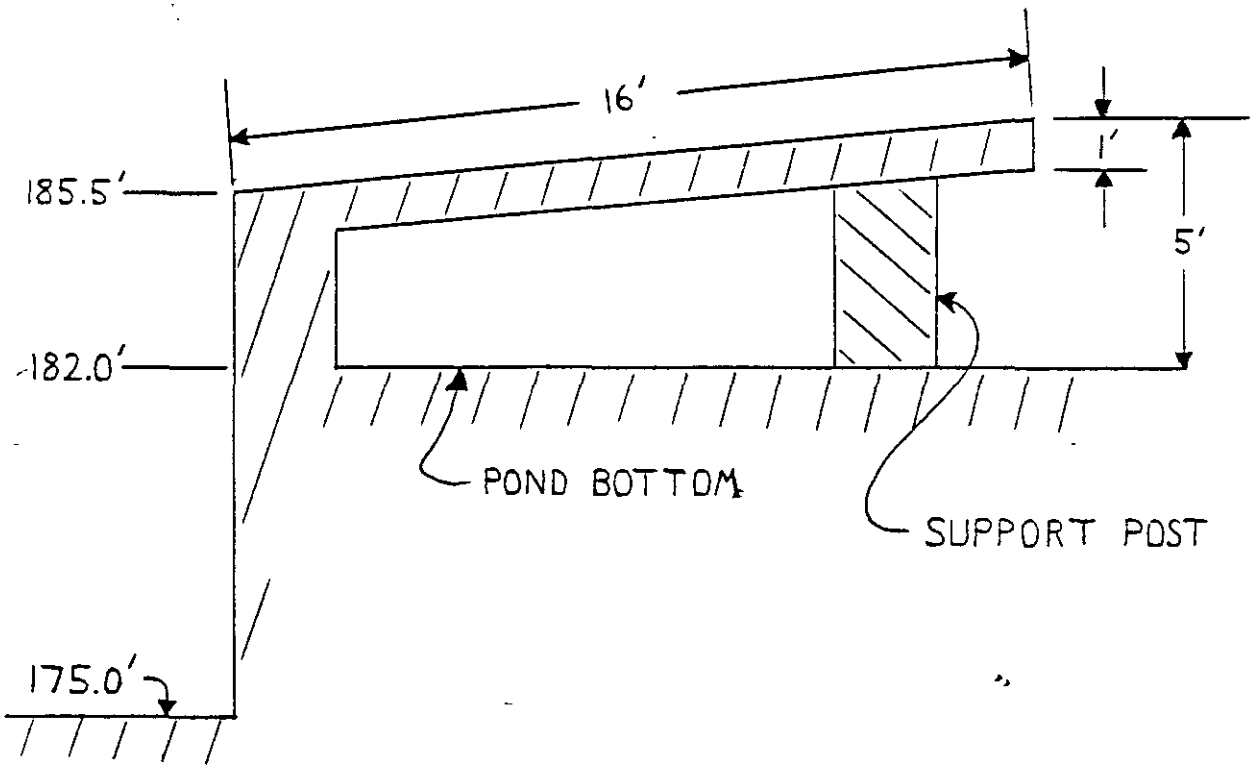

Figure 15. Recommended modification to the L-area outfall design of Fig 3.

APPENDIX A

DIMENSIONAL ANALYSIS OF EQUATIONS

In order to describe heat and momentum transport in a single phase Newtonian fluid, one requires the equations of continuity, momentum, and energy. The presentation and manipulation of the conservation equations is performed here in a cursory manner; for further detail, a text on continuum mechanics should be consulted. The equations are written

$$\begin{aligned} \nabla \rho \mathbf{v} &= 0 \\ \rho \mathbf{v} \cdot \nabla \mathbf{v} &= -\nabla p + \mu \nabla^2 \mathbf{v} - \rho g \\ \rho C \mathbf{v} \cdot \nabla T &= k \nabla^2 T \end{aligned}$$

These equations defy general solution; a common approximation for buoyancy-driven flows in near-incompressible fluids is to neglect variations of density in all but the gravity term. The variation of density with temperature may be described (over reasonable ranges) by

$$\rho = \rho_o \left(1 - \beta (T - T_o)\right)$$

where T_o is a reference temperature at which $\rho = \rho_o$. Rewriting the conservation equations, there results

$$\begin{aligned} \nabla \mathbf{v} &= 0 \\ \rho_o \mathbf{v} \cdot \nabla \mathbf{v} &= -\nabla P + \mu \nabla^2 \mathbf{v} + \rho_o \beta (T - T_o) g \\ \rho_o C_v \cdot \nabla T &= k \nabla^2 T \end{aligned}$$

where

$$\nabla P = \nabla p + \rho_o g$$

P is the static pressure modified to include hydrostatic effects.

Now suitable reference scales may be selected and the terms non-dimensionalized as follows

$\nabla^* \equiv H \nabla$ — H = reference length

$\mathbf{v}^* \equiv \frac{\mathbf{v}}{V}$ — V = reference velocity

$\theta \equiv \frac{T - T_o}{\Delta T}$ — T reference temperature

$P^* \equiv \frac{P}{\rho_o V^2}$ — ΔT = reference temperature difference

$g^* \equiv \frac{g}{g}$ — g = acceleration due to gravity

Substituting into the conservation equations and collecting terms, there results

$$\nabla^* \cdot \mathbf{v}^* = 0$$

$$\mathbf{v}^* \cdot \nabla^* \mathbf{v}^* = -\nabla^* P^* + \frac{1}{Re} \nabla^{*2} \mathbf{v}^* + \frac{1}{Fr} \theta \, g^*$$

$$\mathbf{v}^* \cdot \nabla^* \theta = \frac{1}{Re} \frac{1}{Pr} \nabla^{*2} \theta$$

where

$$Re \equiv \frac{HV\rho_o}{\mu}$$

$$Pr \equiv \frac{C\mu}{k}$$

$$Fr \equiv \frac{V^2}{\beta \Delta T g H}$$

The Reynolds and Prandtl numbers may alternatively be written in terms of the kinematic viscosity as in the text of the report. The Froude number may be modified as follows. Recall

$$\rho = \rho_o(1 - \beta(T - T_o))$$

Then

$$\beta(T - T_o) = \frac{\rho_o - \rho}{\rho_o}$$

From this the Froude number can be written

$$Fr = \frac{\rho_o V^2}{(\rho_o - \rho)gH}$$

where ρ is the density at temperature T.

APPENDIX B

DILUTION IN THE MIXING ZONE

Consider overall balances on the mixing zone of the cooling lake shown in Fig 16. There are three flowing streams involved; the inlet and underflow streams enter, and the mixed stream comes out. If D_v is defined as in Fig 16, all streams may be expressed in terms of the inlet flow Q:

inlet	Q
underflow	$(D_v - 1)Q$
mixed	D_vQ

If all this flow takes place in directions normal to the outfall (this is a reasonable approximation for this experiment), the following heat balance can be written. Heat loss to the environment is neglected.

inlet + underflow = mixed

$$Q\rho C(T_i - T_r) + \int_0^{h_o} vW\rho C(T_b - T_r)dz = \int_{h_o}^{H} vW\rho C(T - T_r)dz$$

W is the width of the channel, h_o is the position of zero velocity, and T_r is a reference temperature. Other terms are defined in the text of the report. If T_r is set to T_b, and the variation of ρ with temperature is neglected, then

$$\frac{Q}{WH}(T_i - T_b) = \int_{\alpha}^{1} v(T - T_b)d\eta$$

where

$$\eta \equiv \frac{z}{H}$$

$$\alpha \equiv \frac{h_o}{H}$$

If the lake flow outside the mixing zone is assumed to be laminar, the velocity profile of the mixed stream can be shown to be

$$v = \frac{3D_vQ}{2WH} \quad \frac{(\eta - \alpha)(\eta + \alpha - 2)}{(\alpha^3 - 3\alpha^2 + 3\alpha - 1)}$$

(Dye injected into this region of the pond was not observed to undergo a rapid dispersion, characteristic of turbulence; however,

the streamlines were often unsteady, more complicated than the one-dimensional flow assumed in this analysis. The equation shown above should therefore be considered a reasonable first approximation to the actual velocity profile.) Substituting this into the energy balance and rearranging terms results in

$$D_v = \frac{T_i - T_b}{T_m - T_b} \; C_m$$

in which D_v as defined in the text of the report is here multiplied by a "mixing correction factor."

$$C_m \equiv \frac{2\,(\alpha^3 - 3\alpha^2 + 3\alpha - 1)}{3\int_{\alpha}^{1} (\eta^2 - 2\eta - \alpha^2 + 2\alpha)\,\frac{T - T_b}{T_m - T_b}\,d\eta}$$

The actual value of D_v depends on the temperature profile in the mixed stream. As T approaches a constant T_m for $\alpha < \eta < 1$, C_m approaches 1.

Suppose that the profile can be described by an equation of the form

$$\frac{T - T_b}{T_m - t_b} = 1 - e^{-c(\eta - \alpha)}$$

where c is a constant of magnitude about 5, such that the exponential function goes to 0 as η approaches 1. Then it can be found that

$$C_m = \frac{\frac{\alpha^3}{3} - \alpha^2 + \alpha - \frac{1}{3}}{(\frac{\alpha^3}{3} - \alpha^2 + \alpha - \frac{1}{3}) + (\frac{1}{c^3} - \frac{1}{2c} + \frac{\alpha}{c} - \frac{\alpha^2}{2c})e^{-c(1-\alpha)} + (\frac{1}{c^2} - \frac{\alpha}{c^2} - \frac{1}{c^3})}$$

Detailed measurements of the vertical temperature profile were taken at a location outside the mixing zone. These data were examined and reasonable values of α and c chosen. These were then used to calculate the correction factor C_m as described above. A typical set of data appears in Fig 17. α and c were chosen to be 0.22 and 5.9; using these, C_m was calculated to be 1.12. For several operating conditions and outfall weir geometries, C_m ranged from 1.06 to 1.12. Since these values are not greatly different from 1, and since they do not vary greatly from run to run, it was decided to calculate and use uncorrected values of D_v, as defined in the text of the report. These, while all about 10% too small, are sufficient to discriminate among different outfall designs.

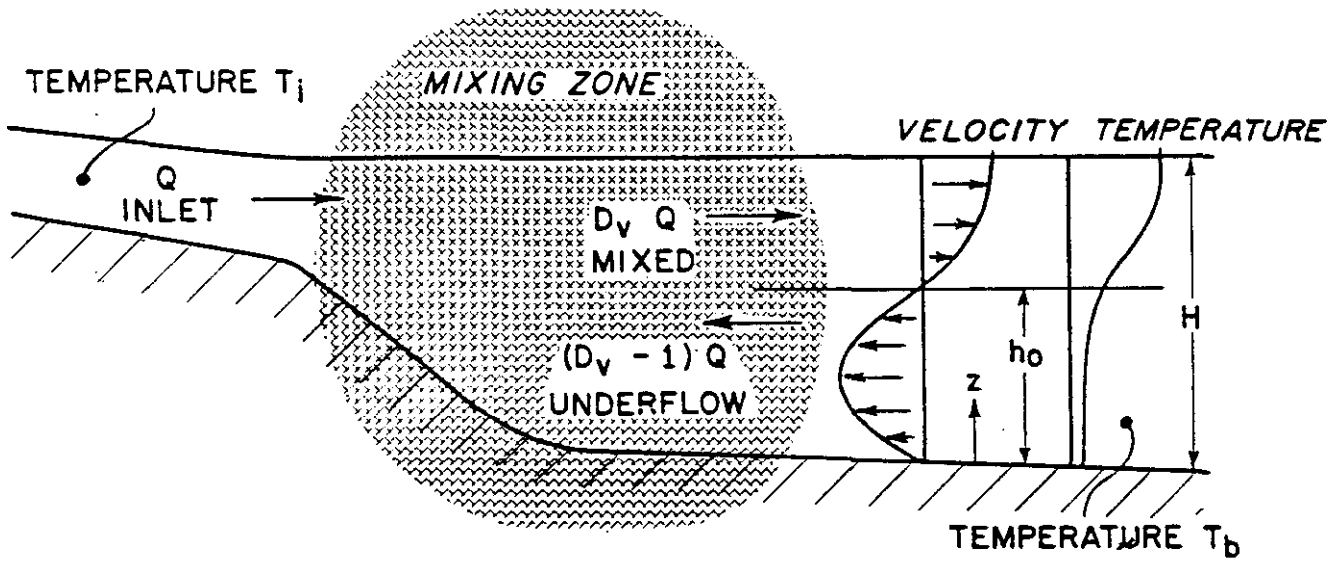

Figure 16. Thermal and hydraulic behavior of a cooling lake.

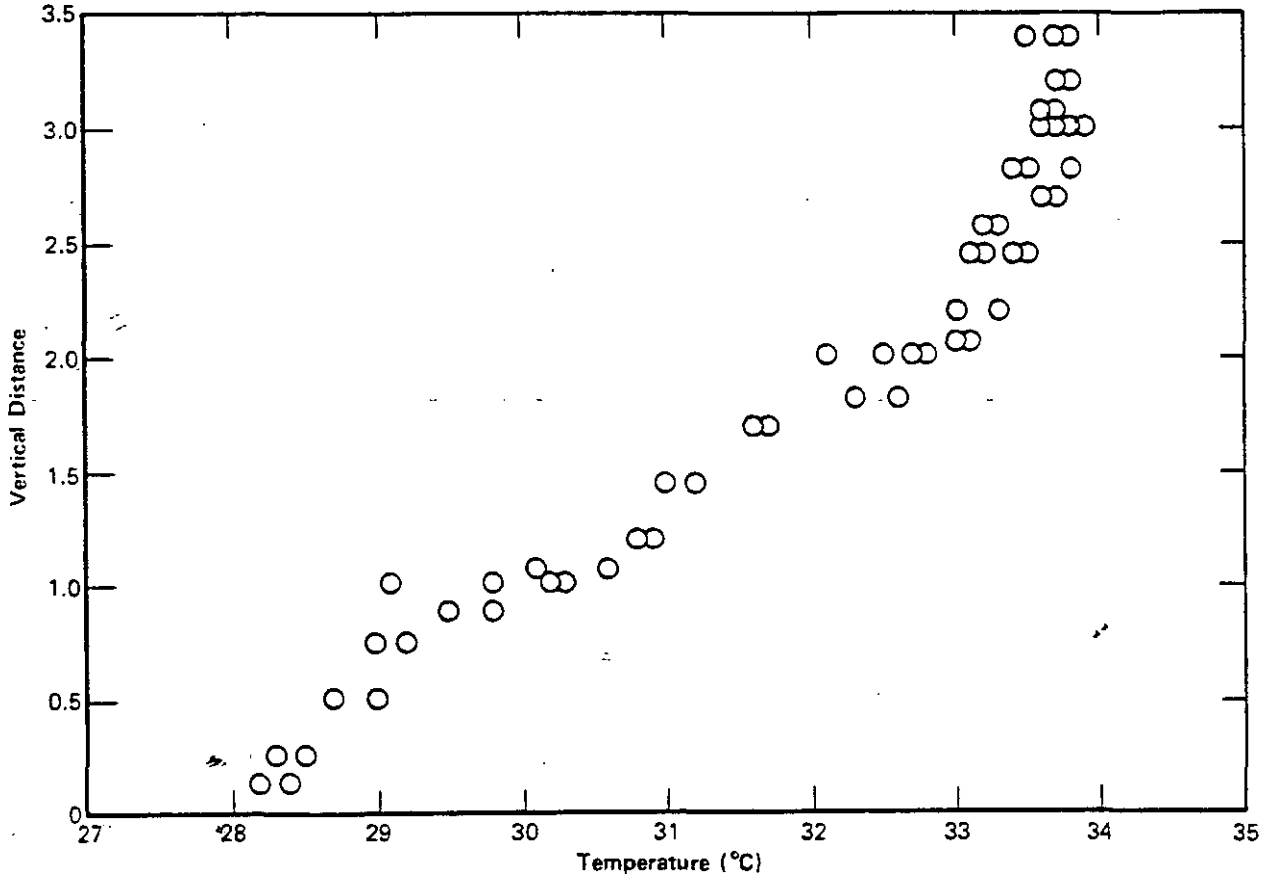

Figure 17. Vertical temperature profile in model pond.